

K. R. Preswath, M. T. Behnam and G. J. Roehrn

Sandia Laboratories, Albuquerque, New Mexico 87185, USA

MASTERABSTRACT

Inertial confinement fusion (ICF) reactors will require driver systems operating with tens to hundreds of megawatts of average power. The pulse power technology that will be required to build such drivers is in a primitive state of development. Recent developments in repetitive pulse power are discussed. A high-voltage transformer has been developed and operated at 3 MW in a single pulse experiment and is being tested at 1.5 MW, 5 kJ and 10 pps. A low-loss, 1 MW, 10 kJ, 10 pps Marx generator is being tested. Test results from gas-dynamic spark gaps that operate both in the 100 kV and 700 kV range are reported. A 250 kV, 1.5 kJ/cm², 30 ns electron beam diode has operated stably for 1.6×10^5 pulses.

INTRODUCTION

Inertial confinement fusion systems require hundreds of kilojoules to be deposited in a few millimeter diameter pellet in approximately 10 ns to achieve significant energy gain from a thermonuclear reaction.¹ Although these high peak power and energy requirements represent a formidable challenge to the pulse power community, significant progress is currently being made for single-shot drivers. After techniques to produce energy gain from thermonuclear pellets are established, repetitive pulse power drivers will be required to provide energy sources for the many ICF experimental programs leading to an economically feasible power plant.

These systems will require 0.5-30 MW of average beam power delivered to the target.² Pellet injection, reactor chamber conditions and economics will limit the pulse repetition rate between 0.1-20 pps. Essentially all of the ICF drivers require electron or ion beams either as the final energy source or as an intermediate step, (gas lasers). At the present time, a few repetitively-operated, pulse power driven, intense beam systems have operated with average powers of 30 kW or less.³

A small research and development effort at Sandia is extending the repetitive pulse power technology to the several megawatts average power level that will be needed for ICF. Recent results on efficient transformer systems, low-loss Marx generators, spark gap switches and cold-cathode diodes are detailed in this paper.

*This work was supported by the U.S. Dept. of Energy, under Contract

NOTICE
This report was prepared as the result of work sponsored by the United States Government. It is hereby stated that the United States Government has certain rights in this report. Reproduction and distribution of this report is unlimited. For sale by the National Technical Information Service, Springfield, MA 01104. Price: MF01/PC02. POSTAGE AND FEE PAID BY ADDRESSEE. POSTMASTER: Send address changes in this report to Sandia Laboratories, Albuquerque, New Mexico 87185. This report is available for sale by the National Technical Information Service, Springfield, MA 01104. Price: MF01/PC02. POSTAGE AND FEE PAID BY ADDRESSEE. POSTMASTER: Send address changes in this report to Sandia Laboratories, Albuquerque, New Mexico 87185.

HIGH-VOLTAGE TRANSFORMER SYSTEMS

Air-core transformers operating in a dual-resonance circuit provide an efficient method for charging high-voltage, pulse forming transmission lines (PFL). A ring-shielded, spiral strip transformer design was developed during the past few years at Sandia Laboratories.⁴ One of these transformers has operated in the 500-700 kV voltage range at 10-100 pps for $> 2 \times 10^7$ pulses without any damage.^{5,6} Recently, another transformer produced 3 MV output voltages on a single pulse operation⁷ and is being tested up to 1.5 MV and 10-20 pps.

Spiral strip transformers are better suited to PFL charging than their helical wound counterparts because they are less vulnerable to interturn dielectric breakdown from nanosecond voltage transients fed back into the transformer secondary when the PFL discharges. The spiral strip winding has an optimum interturn series capacitance distribution between the output and ground which produces a uniform electric field gradient during the fast transient voltage pulses. Substantial field enhancement occurs at the edges of the 0.25 mm thick secondary winding unless an electric field grading structure is added to both the case and the core. The ring cage grading structure shown in Fig. 1 produces nearly uniform electric fields in the margin of the windings without disrupting the magnetic coupling of the transformer.⁴

The transformer shown in cross section in Fig. 1 has a single turn primary surrounding a 42 turn secondary winding. It has been tested to 3 MV in a dual-resonance charging arrangement using the test assembly sketched in Fig. 2.⁷ The voltage is stepped-up from 30 kV (± 4.5 kV) on the two 1.85 μ F primary capacitors to 3 MV on the 0.76 nF water-dielectric capacitor with a 91 percent energy transfer efficiency. The output voltage waveform is dual-polarity and the total energy transfer time is 3 μ s. The mean dielectric stress in the oil-polyester insulation of the secondary winding is 470 kV/cm at 3 MV.

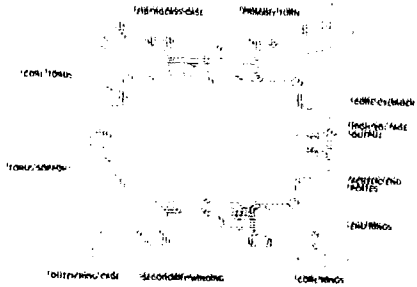


Fig. 1. Three megavolt transformer.

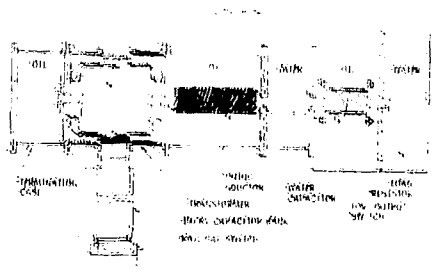


Fig. 2. Cross section of three megavolt transformer test assembly.

The test assembly has been modified for changing a 4 nF output capacitor to 1.5 nF at 10 pps. The transformer has been operated at 0.75 MW and 20 pps for 10^5 pulses in a single run without any problems. The 91 percent energy transfer efficiency is maintained in the repetitive operation. Less than one percent of the stored energy is dissipated in the transformer. This loss results in joule heating of the transformer primary. An approximate relationship between the primary and secondary joule heating losses is given by equation (1)

$$\frac{I_p^2 R_s}{I_p^2 R_p} \sim \frac{n^2 V_s^2}{(V_s/nV_p)^2 R_p} \quad (1)$$

where R_s and R_p are the primary and secondary resistivities, V_s is the secondary voltage, V_p the primary voltage, and n the turns ratio. For a transformer with a gain of 30 and a 42:1 turns ratio, the secondary losses are less than 5 percent of the primary losses.

Gas-dynamic spark gaps are being developed for the primary circuit switch in repetitive operation. Two configurations that have been tested are the rail switch⁶ and the cylindrical flat-button spark gap⁸ shown in Figs. 3 and 4, respectively. The rail gap has been operated on the 300 J RIF-I for sustained runs as long as 10^6 shots at 11 kA. Breakdown rates with brass electrodes that are cooled by flowing air^{5,6} are 50 $\mu\text{g}/\text{cm}^2$ with a 5.8 μs energy transfer time. This switch has a wide triggering range. It will trigger at less than 30 percent of the self-breakdown voltage and does not malfunction with extensive electrode erosion. In another experiment, a slightly modified version was operated with the main electrodes cooled by water.⁸ With the air flow adjusted for stable operation ($\ll 1$ prefire in 10^3 shots) 40 percent of the energy dissipated in the switch was carried away by the cooling water and 60 percent by the air flowing through the trigger electrode.

Since the charge transfer per pulse through these switches is relatively high for repetitive operation and will increase substantially as primary energy storage

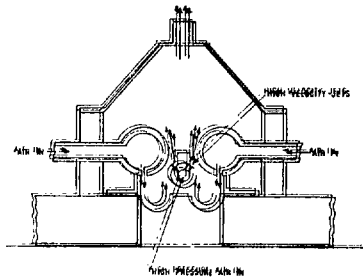


Fig. 3. Rail gap switch.

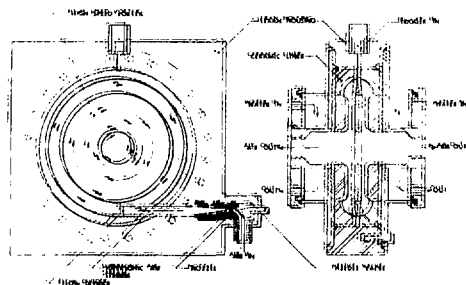


Fig. 4. Cylindrical flat-button, three-electrode spark gap.

is increased, it is necessary to maximize the electrode area to achieve long switch lifetimes. The electrode area can be increased more than an order of magnitude over the rail switch with the flat-button spark gap. The switch also has a wide triggering range and a low prefire rate.⁸ The flowing gas is used more effectively for cooling this switch and restoring its dielectric strength. A version of this spark gap with 10 cm diameter copper electrodes is presently being tested on the 1.5 MV transformer experiment. The arcs occur uniformly over the electrode area and with $\sim 10^5$ pulses at ± 15 kV and 420 J/pulse, the electrode material erosion was not sufficient to cause a detectable change in the electrode gap spacing.

REPETITIVELY PULSED MARK GENERATOR

Mark generators are also being investigated as a possible primary energy storage element in high average power accelerators. In repetitive applications, the Mark generator should operate with 90-95 percent efficiency for $\sim 10^9$ pulses with low prefire rates ($\ll 1$ prepulse in 10^4 pulses). Circuit calculations indicate that the high energy-transfer efficiency can be achieved with an inductively-isolated Mark circuit.⁹ A 1 MV, 10 kJ, 10 pps inductively isolated Mark generator has been designed, fabricated and is presently undergoing test. Figures 5 and 6 are a schematic diagram and a photograph of this generator during assembly. A 4 Ω resistor has been added in series with the 135 μ H inductors to dissipate the energy left stored in these inductors after the Mark discharges. The generator has ± 65 kV charging for the capacitors and 130 kV, 50 kA spark gaps with coaxial electrodes as sketched in Fig. 7. Two arcs occur from the trigger electrode on each pulse.

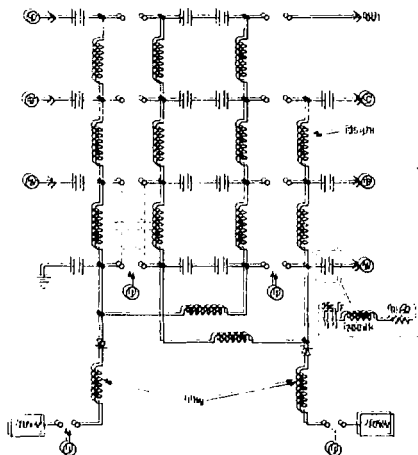


Fig. 5. Schematic diagram of 1 MV, 10 kJ, 10 pps Mark generator.

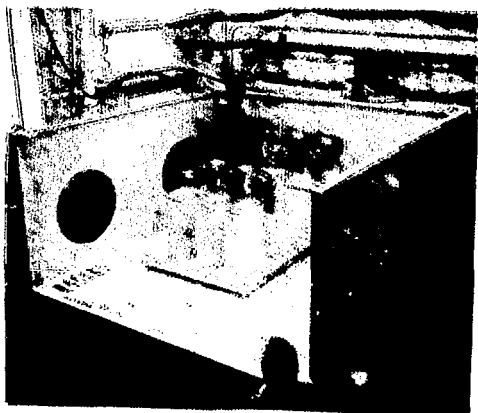


Fig. 6. Photograph of 1 MV, 10 kJ, 10 pps Mark generator during assembly.

The interelectrode capacitance is high because efforts have been made to substantially increase the useful electrode area. The electrodes are cooled by both air (or SF₆) and water. The water flows through the isolating inductors and trigger resistors. Although the generator is connected in an $n = 2$ capacitive coupled arrangement,¹⁰ the triggering range was extremely small due to the large interelectrode capacitance of the spark gaps. One kilo-ohm resistors were added between the trigger electrode and two stages back to convert it to a resistively coupled Marx generator. With this arrangement the Marx generator has been triggered as low as 60 percent of the self-breakdown voltage. The resistors result in an additional energy loss of 1-2 percent for this generator. At the present time the Marx generator has been operated at half voltage at 5 pps for about 300 pulses per run into a resistive load.

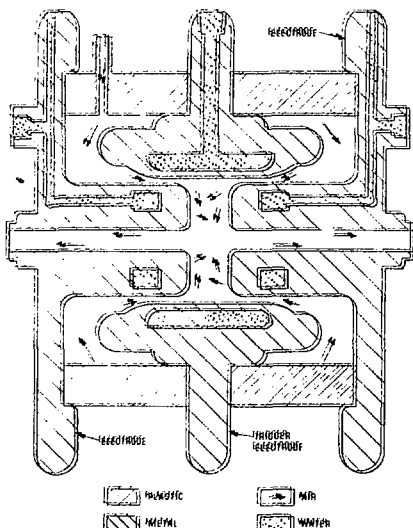


Fig. 7. High power Marx generator spark gap.

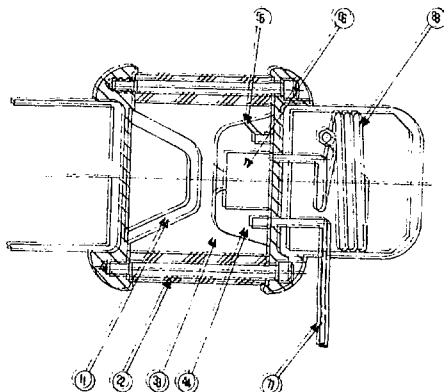


Fig. 8. High voltage spark gap. 1 and 4 are electrodes, 2 is the acrylic housing, 3 is high pressure gas region, 5 and 7 are gas inlets, 6 and 8 are air outlets.

HIGH VOLTAGE SPARK GAPS

Transformers or Marx generators will change PFM's in high average power generators. Multichannel gas-dynamic, spark gaps are the most promising switches to provide the high-voltage, high current, low-jitter and long lifetime operation required for switching the transmission lines. Initial investigation of the properties of two-electrode spark gaps are being made on KMP-1.^{5,6} A 700 kV, 20 kA spark gap (see Fig. 8) is installed in this facility. It has operated at 30 kW

average power for durations of 3×10^4 pulses and at 530 kV, 11 kA, 40 nps for 10^6 pulses in a single run. A dual-polarity voltage waveform, shown in Fig. 9 is applied to the switch. In a 10^6 pulse run the air flow was adjusted for stable operation at 16 l/s. The time between when the voltage became 100 kV positive until the time when breakdown voltage occurred for each pulse was measured and the histogram in Fig. 10 was generated.¹¹ A normal distribution with a standard deviation of 44 ns fits this histogram and prefires outside of this distribution did not occur. This time jitter corresponds to a 1.8 percent rms spread in breakdown voltage (see Fig. 9). The erosion of the tungsten alloy electrodes was about 500 $\mu\text{g}/\text{C}$ during this run.^{5,6} With the 30 ns pulse duration 6.3×10^{-4} C/pulse were transferred and the expected lifetime of the switch is greater than 10^9 pulses.

In a 30 kJ electron beam accelerator (a possible size of a single reactor module), each arc channel of the gas switches will pass 2-10 kJ depending upon the switch inductance, pulse risetime and pulse duration. The electrodes in these higher energy switches could easily have a factor of four larger area than the RFP-I switch. This larger area and the higher voltage (~ 2 MV) operation (with subsequent lower charges per unit energy) implies that the lifetime of larger energy switches could be within an order of a reactor scenario.²

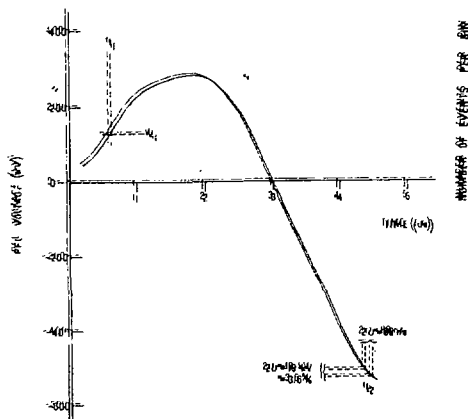


FIG. 9. PPE charge voltage waveforms.

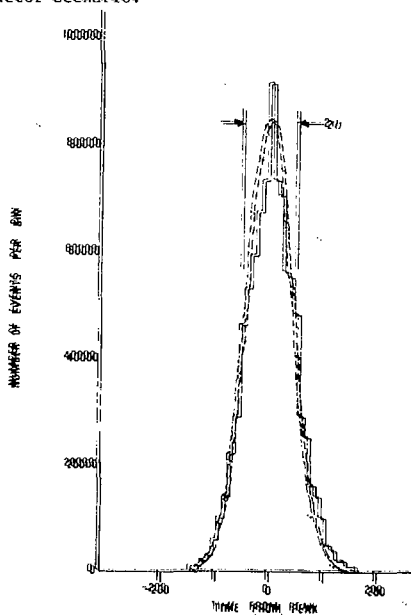


FIG. 10. Histogram of the 700 kV switch breakdown times.

GOLD CATHODE DIODES

Another area of concern for high-average power electrons and ion beam accelerators is the pulse-to-pulse reproducibility and long term stability of the cold-cathode diode impedance and the effective lifetime of these cathodes. Three cathode configurations operating at 250 kV, $\sim 1 \text{ kA/cm}^2$, 30 ns have been tested for extended runs (20,000-160,000 pulses) to explore these issues. In these experiments the voltage and current waveforms were digitally sampled at 4 ns intervals and the data for each shot was computer processed and stored on tape.⁹ Pulse waveforms were generated using the average value of the voltage, current and impedance for each time step for a selected number of shots to compare the data either during or after the experiment.

In the first experiment a cross hatched cathode was tested for 20,000 shots at a pulse repetition frequency (PRF) of 10 Hz. Less than 3 percent change in voltage or current occurred throughout the test duration¹³ until the diode shorted. Although the average current density was approximately 1 kA/cm^2 , emission was much higher on field enhanced corners of the cross hatching. These points were reproduced on the anode by hemlets which drilled a corresponding pattern of holes. The run was terminated when one of these holes completely penetrated the 3 mm thick aluminum anode and the diode shorted.

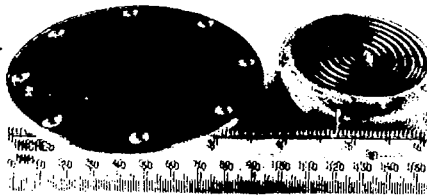


Fig. 11. Anode (left) and cathode for 157,000 shot run.



(a)



(b)

Fig. 12. Waveforms for a ring cathode
a. Aged cathode waveform
(20 ns/cm, upper trace voltage
at 120 kV/div, lower trace
current at 15 kA/div).
b. New cathode, same scales as a.

The grooved, 3 cm diameter brass cathode of Fig. 11 was used to improve beam uniformity. It was operated for 1.6×10^5 pulses without apparent damage. Data were taken at 10 Hz (20,000 shots), 20 Hz (40,000 shots) and 33 Hz (50,000 shots). No anode damage occurred below 33 Hz. At 33 Hz slight anode erosion which replicated the cathode groove pattern was observed.

Typical waveforms are given in Fig. 12 where the upper trace is the voltage and the lower trace is the diode current. Fig. 12b is typical of data taken with a new cathode. The voltage exhibits a spike as cathode plasma forms then drops to a well defined plateau. Current rises slowly during the voltage spike then also has a plateau. Secondary voltage and current plateaus result from the reflected diode voltage during the plasma formation phase. After the diode was pulsed several tens of thousand of times the plasma formation phase becomes longer and the initial voltage increases. The first voltage plateau disappears. The result of this aging process is shown in Fig. 12a. Aging may be reversed by the application of a light coating of diffusion pump oil to the cathode. Fig. 12a is from the first shot after such a coating, Fig. 12b is from the next shot. Apparently carbonization of the oil applied prior to shot 12a provided emission sites for 12b and subsequent shots. As a consequence the aging process was reversed. This cathode subsequently aged at a rate similar to the aging rate of the original cathode.



Fig. 13. Wire roll pin cathode together with anode showing beam damage.

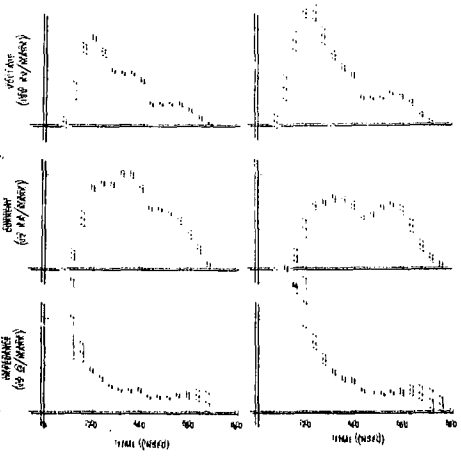


Fig. 14. a. Digitizer output waveforms for a new cathode.
 b. Digitizer output waveforms for an aged cathode.

The third cathode studied (Fig. 13) was made from 1.5 mm hollow metal cylinders (roll pins) mounted on a brass backing. In a run of 10^5 shots it exhibited the same aging observed in the previous cathode. This is illustrated by the digitized waveforms of Fig. 14. The variation previously noted in the current and voltage waveforms are apparent. In addition the impedance waveform is seen to take longer to stabilize in agreement with the retarded plasma formation model.

Shot-to-shot stability is unchanged as the cathode ages. The error bars on Fig. 14 mark one standard deviation of the waveform about the mean value. Typically for the portions of the waveform which do not vary rapidly with time the variation is 3 percent or less. This implies a 4 to 5 percent stability in quantities like impedance, power, and total beam energy.

The roll pin cathode ages more rapidly than the circular groove cathode as shown in Fig. 15. Diode impedance at the peak of the voltage waveform increase roughly twice as rapidly for the roll pin as compared to the grooved cathode. This data shows that cathodes with sharp edged emitters age more rapidly than blunt cathodes. The implication may be that laser diodes which generally employ thin foil emitters will age rapidly in repetitive service and require frequent maintenance.

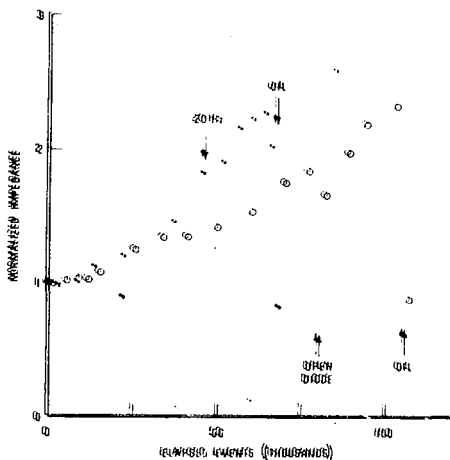


Fig. 15. Change in the diode impedance at voltage maximum vs. accumulated shots. The dots and downward pointing arrow refer to the roll pin cathode. Circles and upward arrows correspond to the ring cathode.

CONCLUSIONS

Experiments to develop the repetitive pulse power technology for ICF drivers are underway. Spiral-strip air core transformer have been operated to 3 MV in a single pulse modes and are being tested to 1.5 MV, 5 kJ, and 10 pps in efficient circuit configurations. Spark gap switches capable of handling the high peak powers in the primary circuit for extended lifetimes are being developed. Inductively coupled Marx generator characteristics are being investigated in a 1 MV, 10 kJ, 10 pps system. A 700 kV spark gap has demonstrated stable operation at 40 pps without prefires with moderate (~ 16 l./i.) flow rates and relatively low electrode erosion rates. Cold cathode diodes show approximately 3 percent shot-to-shot variations in voltage and current but a gradual increase in the turn-on time for greater than 20,000 pulses for three different types of cathodes.

REFERENCES

1. J. H. Nachells, Tech. Digest of Topical Mtg. on Inertial Confinement Fusion, Feb. 7-9, 1978, San Diego, CA, Optical Society of America, Washington, DC.
2. K. R. Prestwich, D. L. Cook and G. Jonas, Trans. of the 2nd Topical Mtg. on the Technology of Controlled Nuclear Fusion, May 9-11, 1978, Santa Fe, NM, p.261.
3. G. J. Rohwein and M. T. Buttram, Preliminary Design of a 100 Hz, 350 kV Short Pulse Generator, Sandia Report SAND77-0174, June 1977.
4. G. J. Rohwein, Development of a 3 MV Transformer to be published in the Proc. of the 2nd Int'l. Pulsed Power Symposium, June 1979, Lubbock, TX.
5. G. J. Rohwein, M. T. Buttram and K. R. Prestwich, 2nd Int'l. Topical Conf. on Electron and Ion Beam Research and Tech., Cornell Univ., Ithaca, NY, Oct. 1977, p.845.
6. M. T. Buttram, G. J. Rohwein, Proc. of the 13th Symposium on High Power Modulators, Buffalo, NY, May 1978, p.303.
7. G. J. Rohwein, Development of a 3 MV Pulse Transformer, Sandia Report SAND79-0813, May 1979.
8. G. J. Rohwein, Fusion Progress Report, SAND79-11011, p.123.
9. M. T. Buttram, *ibid*, p.125.
10. K. R. Prestwich and D. L. Johnson, IEEE Trans. Nucl. Sci., Vol. NS-16, No. 3, June 1969, p.493.
11. M. T. Buttram, Online Data Acquisition System for Repetitive Pulse Development, Sandia Report SAND78-1753, Sept. 1978.
12. Same as Ref. 8, p.129
13. M. T. Buttram, Operation of a Repetitively Pulsed 300 kV, 10 kA Electron Beam Diode, to be published in IEEE Trans. Nucl. Sci., NS-26, No. 3, June 1979.